



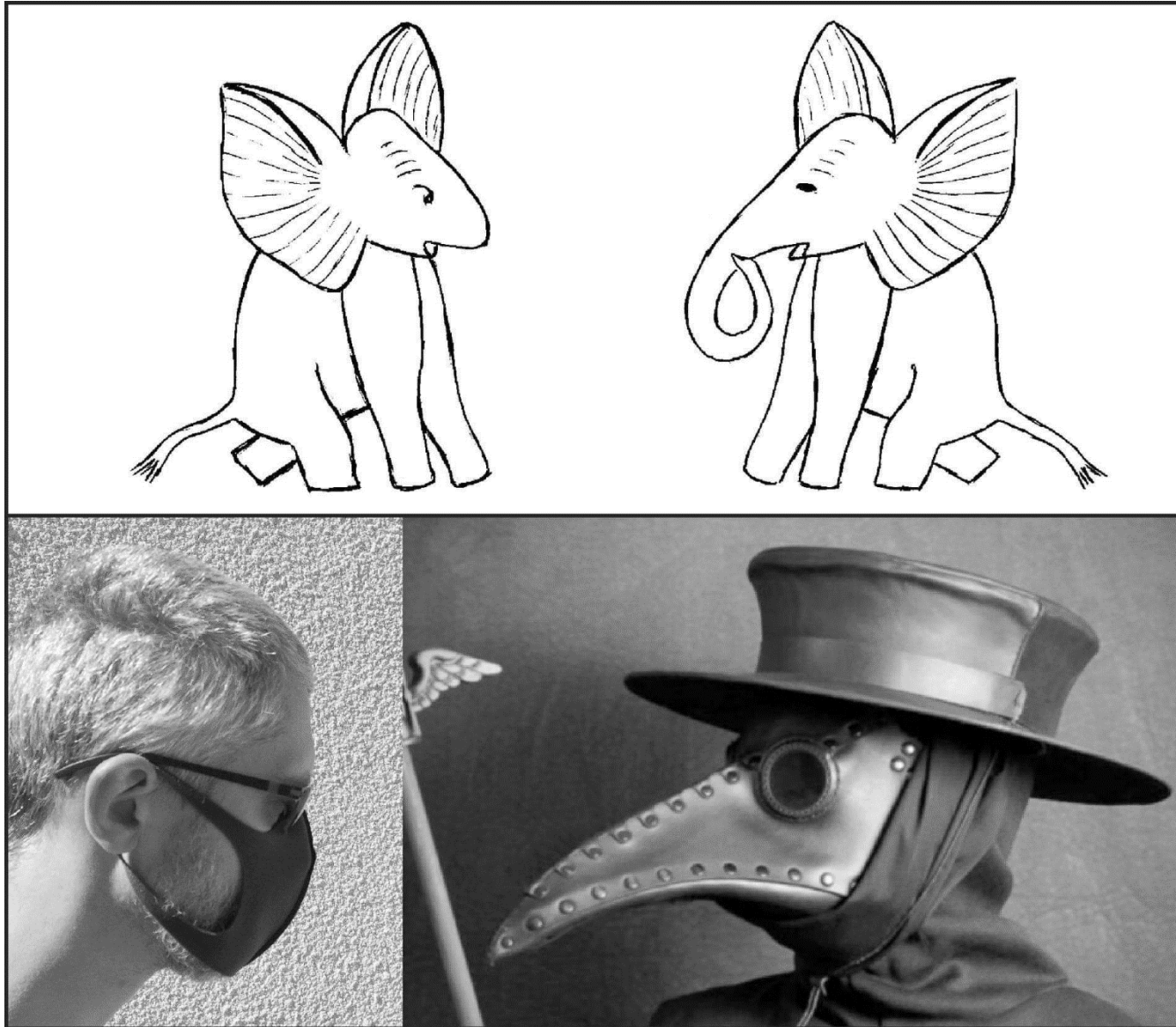
| The European Synchrotron

Electron-phonon interaction as seen in diffuse and inelastic scattering

Alexei Bosak

European Synchrotron Radiation Facility
Grenoble, France

The Elephant's Child et al.



- ✓ Diffuse and inelastic x-ray scattering
- ✓ Bad and good nesting with biased examples

TDS intensity $\sim 1/\omega^2$

$$I(\vec{Q}) \propto \sum_{j=1}^{3N} \frac{1}{\omega_j} \coth\left(\frac{\hbar\omega_j}{2kT}\right) \left| \sum_{d=1}^N f_d(Q) \exp(-W_d(\vec{Q}) + i\vec{Q} \cdot \vec{d})(\vec{Q} \cdot \hat{\sigma}_d^j(\vec{q})) M_d^{-1/2} \right|^2$$

LE JOURNAL DE PHYSIQUE ET LE RADIUM.

SÉRIE VIII, TOME X, MARS 1949.

DIFFUSION DES RAYONS X DANS L'ALUMINIUM PAR LES ONDES D'AGITATION THERMIQUE

Par PH. OLMER.

Assistant à la Faculté des Sciences de Paris.

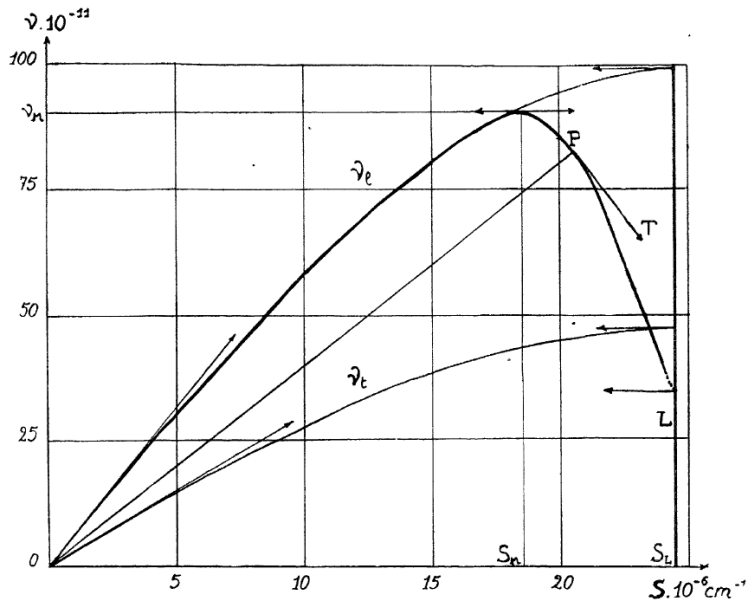


Fig. 13.

X-ray tube + point detector
since 1948

ID28 hardware

beamlines



Synchrotron JSR
JOURNAL OF
SYNCHROTRON
RADIATION

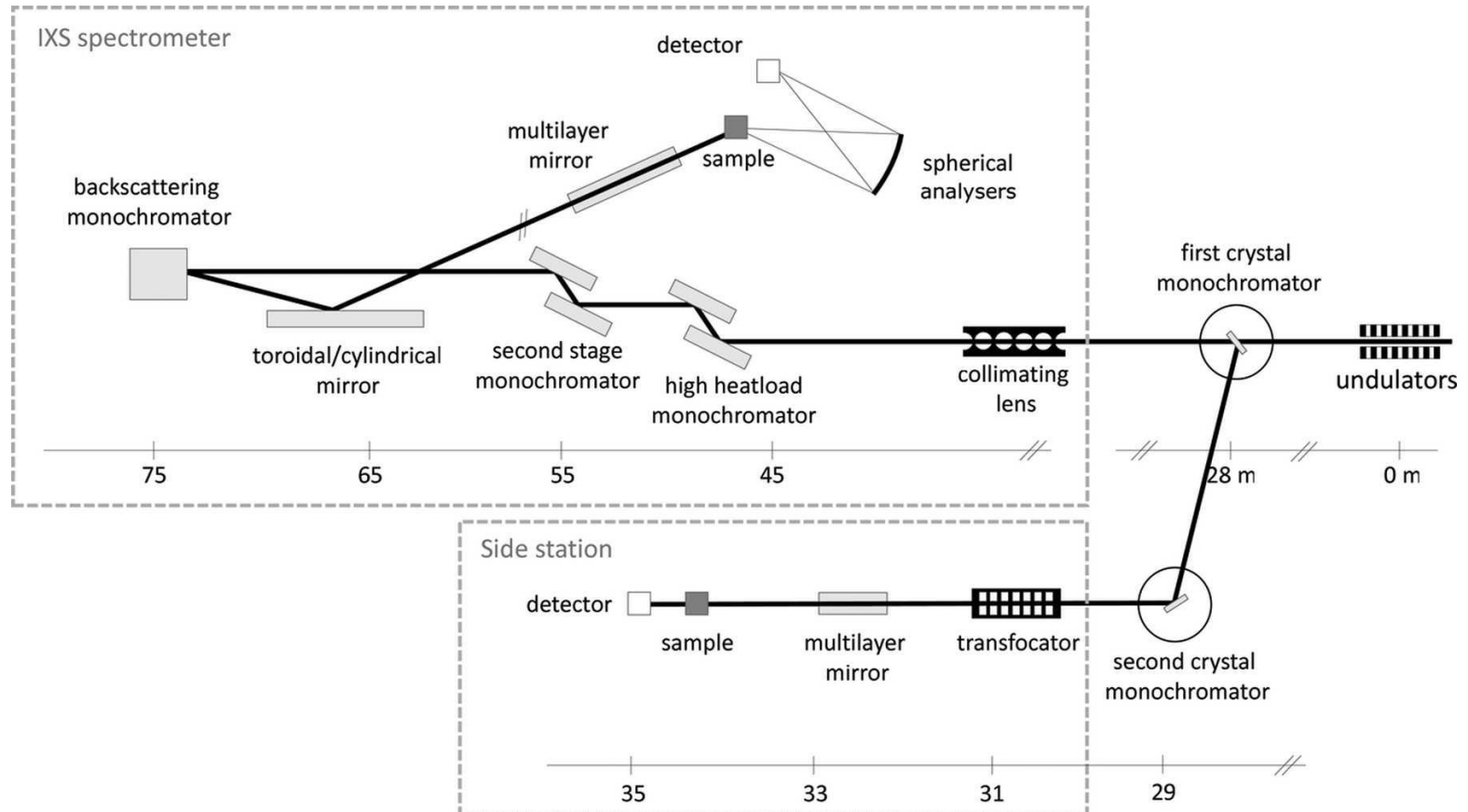
ISSN 1600-5775

**A new diffractometer for diffuse scattering studies
on the ID28 beamline at the ESRF**

**A. Girard,^{a*} T. Nguyen-Thanh,^b S. M. Souliou,^b M. Stekiel,^a W. Morgenroth,^a
L. Paolasini,^b A. Minelli,^b D. Gambetti,^b B. Winkler^a and A. Bosak^{b*}**

Diffuse scattering:

- Roadmaps for IXS measurements
- Identification of diffuse features
- Validation of lattice dynamics/disorder models



New ID28 diffractometer

C(311)[splitter]-Si(422) monochromator

0.52-0.98 Å

flux $\sim 10^{12}$ ph/s @ 17.8 keV

focal spot down to $20 \times 40 \mu\text{m}$

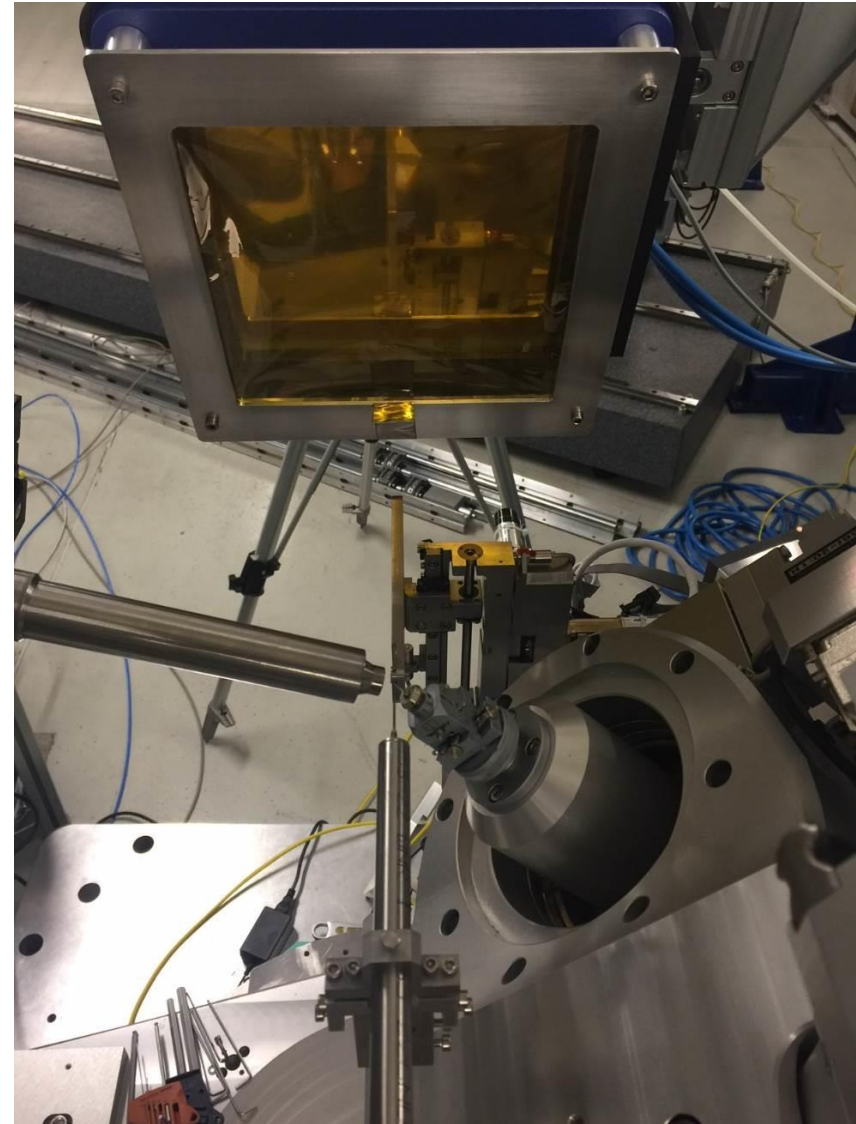


SPONSORED BY THE



Federal Ministry
of Education
and Research

BMBF 05K13RF2

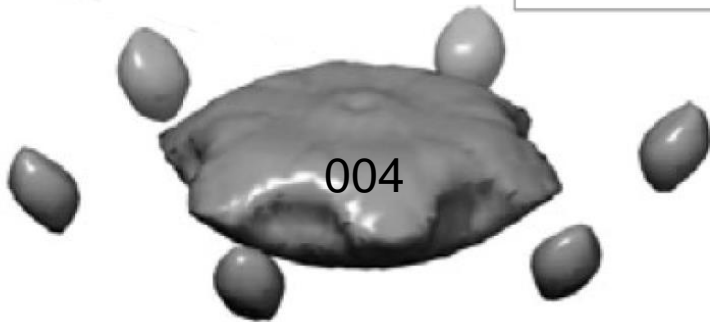
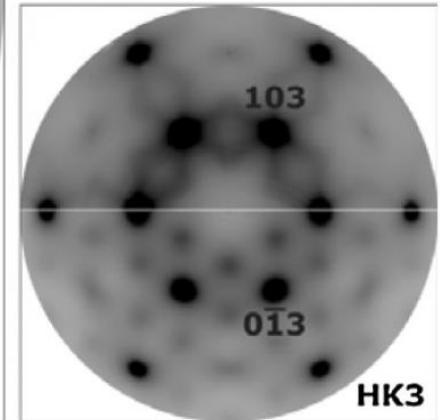
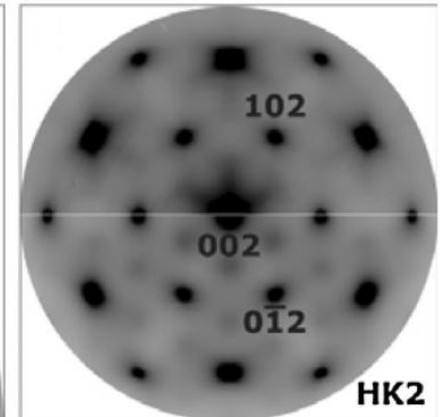
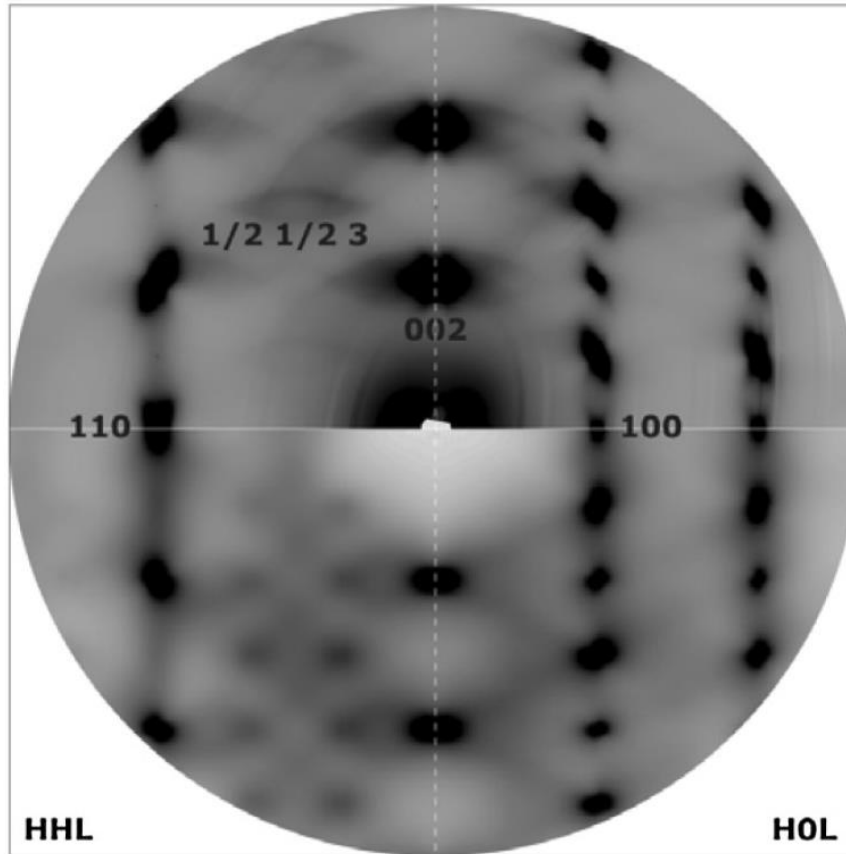
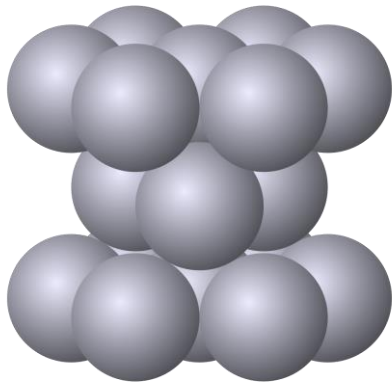


user operation from September 2016

Zinc metal

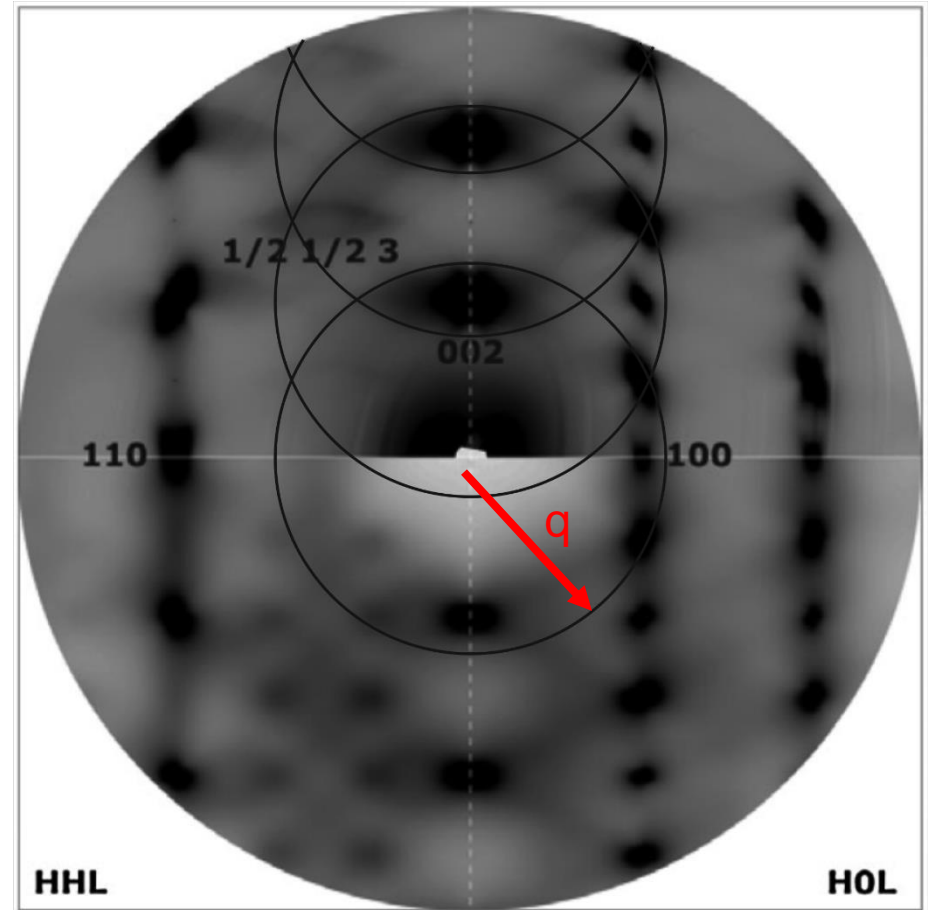
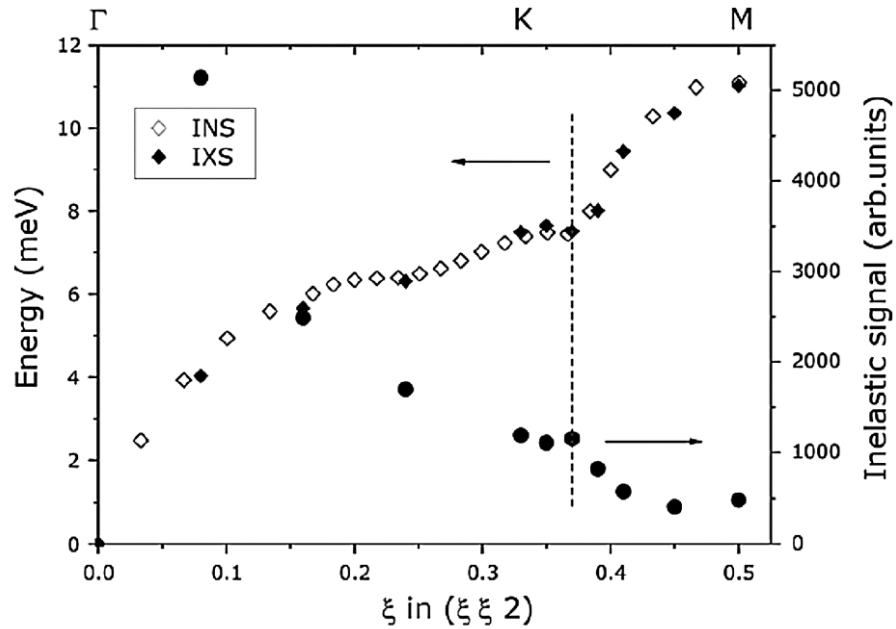
[A. Bosak et al., PRL 103, 076403 (2009)]

Zinc metal



[PRL 103, 076403 (2009), Bosak et al.]

Zinc metal

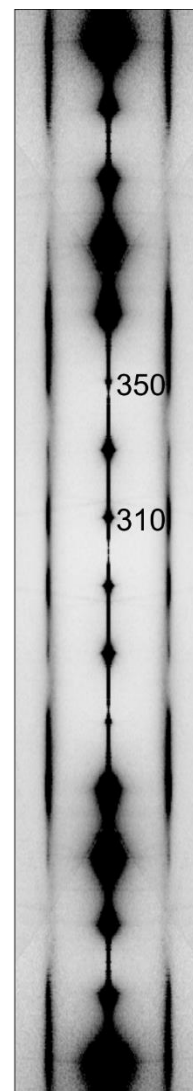
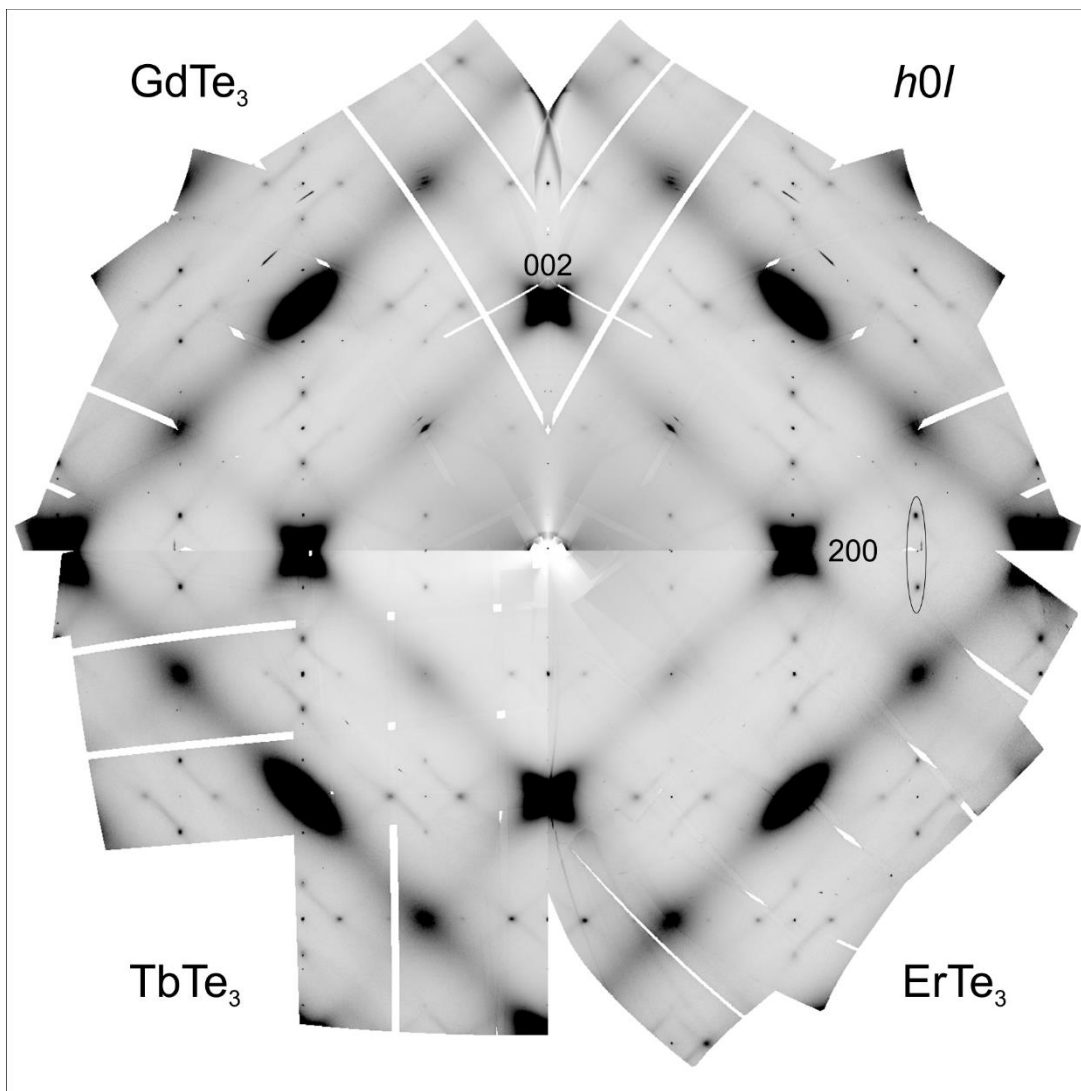


Free electron model:
 $k_F = q/2 = 1.57 \text{ \AA}^{-1}$
 $\Rightarrow 2 \text{ electrons / Zn atom}$



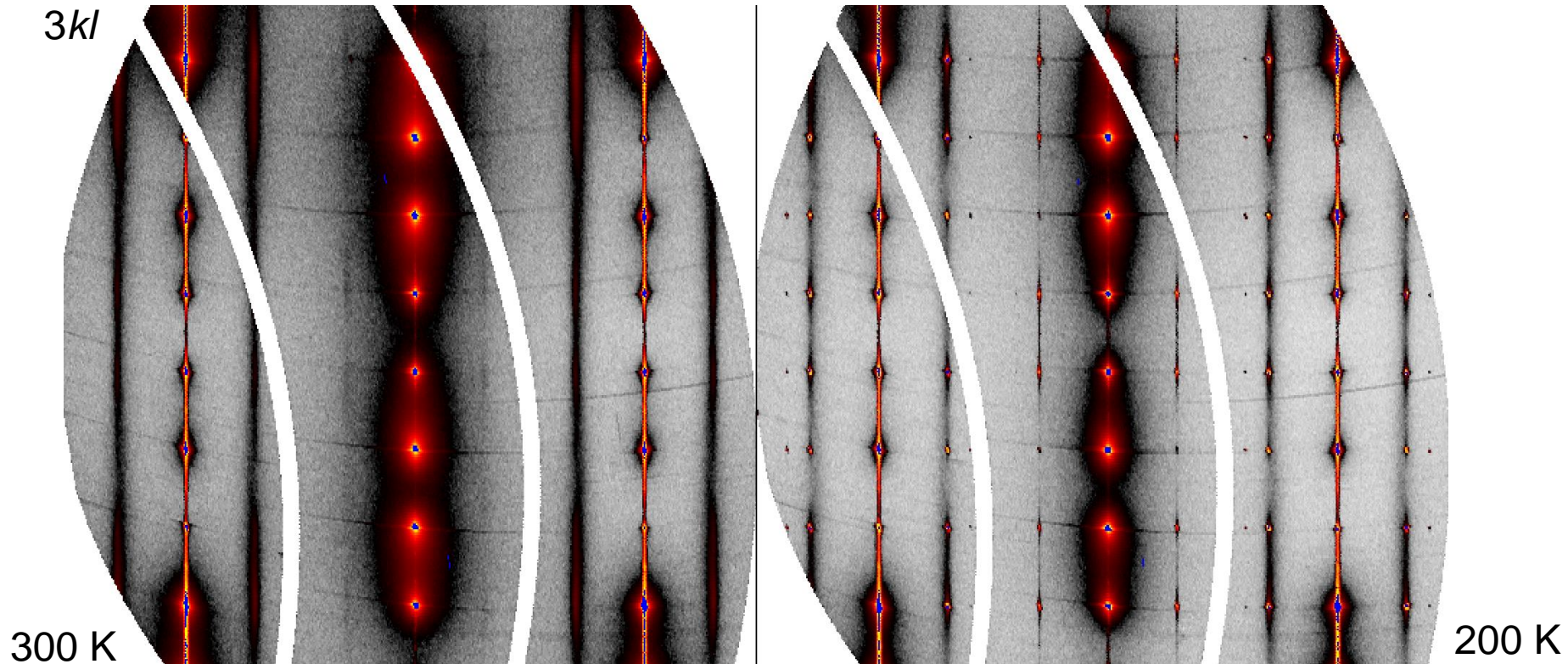
[with P. Quemerais, P. Monceau, E. Lorenzo, P. Rodier,
L. Ortega, A. Sinchenko, E. Bellec]

Diffuse scattering in $R\text{Te}_3$



ErTe_3 , TbTe_3 ,
 GdTe_3 all look the same above T_{CDW}

Diffuse scattering in ErTe_3



- ErTe_3 , TbTe_3 , GdTe_3 all look the same below $T_{\text{CDW}1}$
- Deviation from sinus modulation
- Suspicious contribution from planar defects

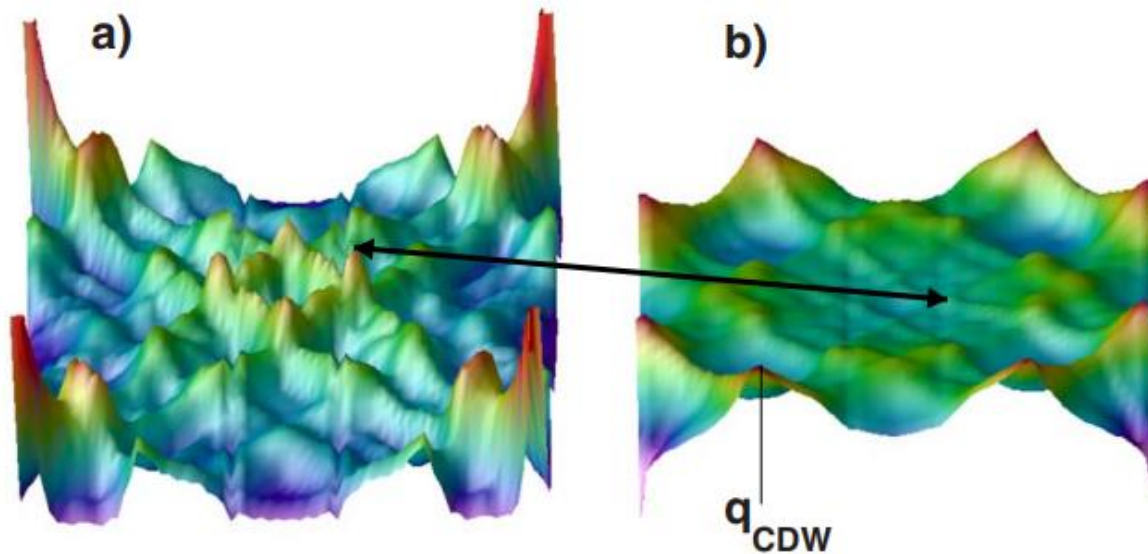
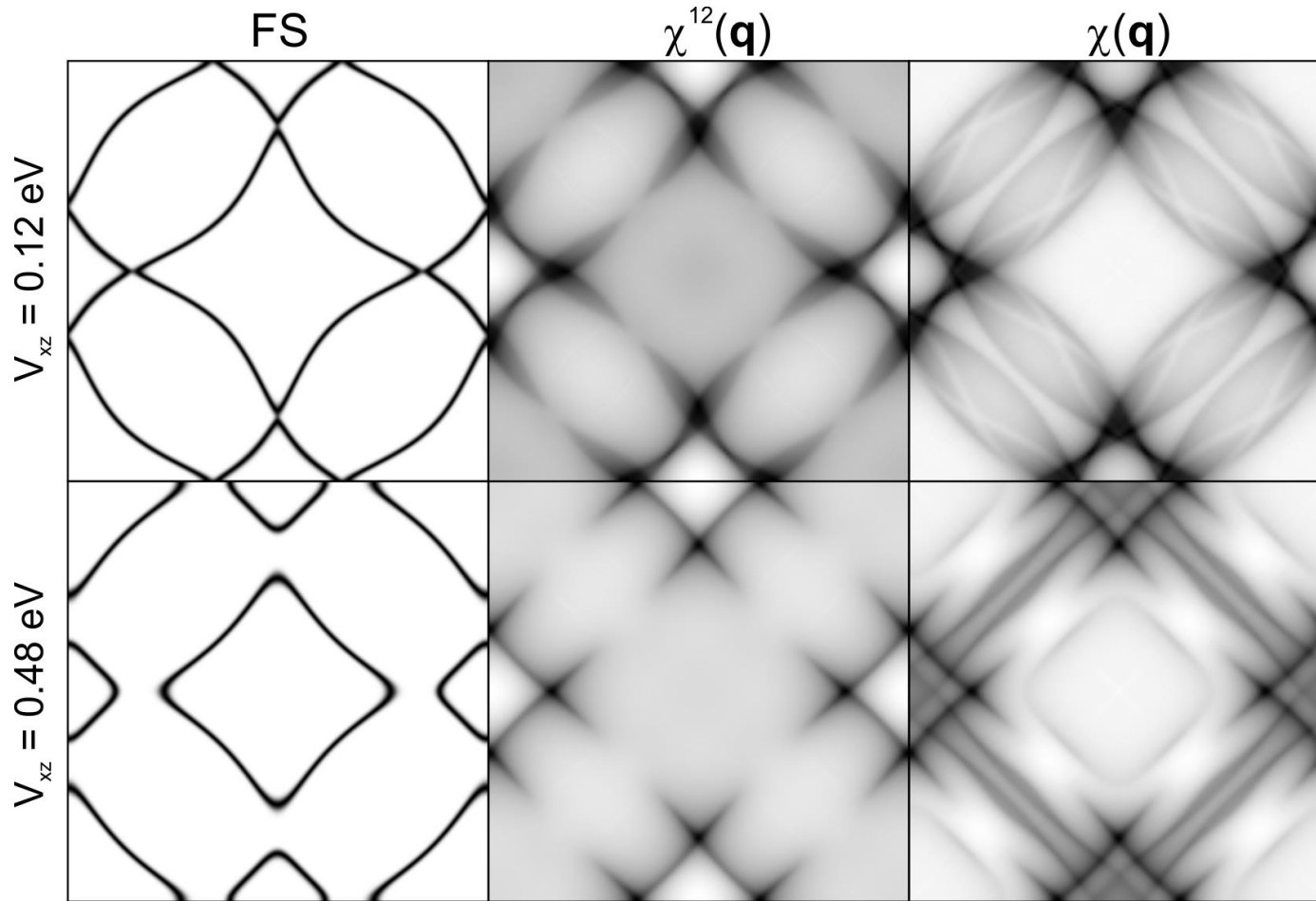


FIG. 6. (Color online) A diagram showing the imaginary (left) and real (right) parts of the susceptibility as a function of q_x, q_y , with $q_z=0$. The arrow connects the strongest peak in the imaginary part, located at \mathbf{q}_{nest} , to its corresponding position in the real part. In the real part, the nesting peak is absent and \mathbf{q}_{CDW} dominates the spectrum, indicating the importance of states away from E_F .

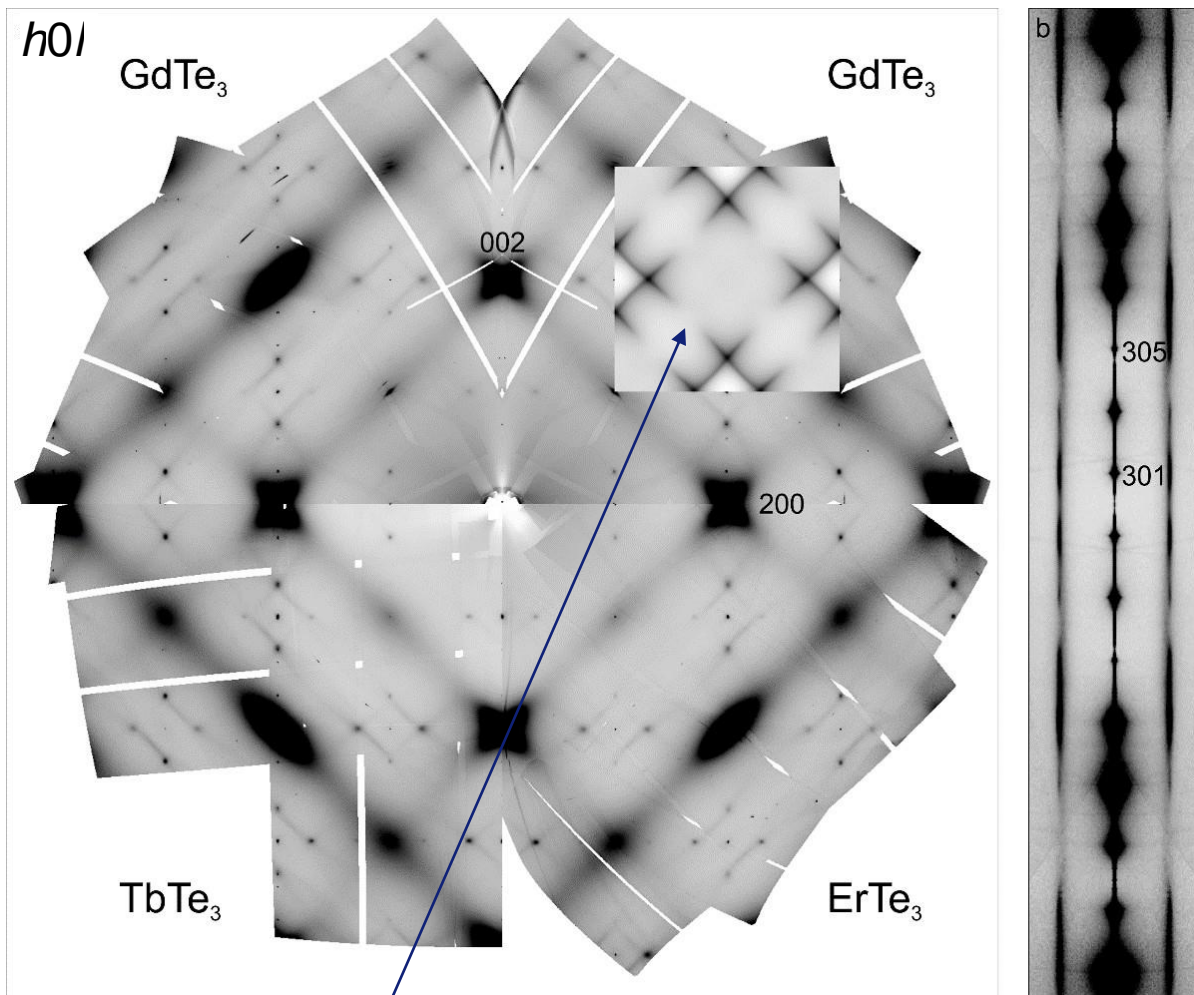
[M.D. Johannes and I.I. Mazin, PRB 77, 165135 (2008)]

$R\text{Te}_3$ - nesting behind CDW



$$\chi^{ij}(\mathbf{q}) = \sum_{\mathbf{k}} \frac{n_F[E^i(\mathbf{k})] - n_F[E^j(\mathbf{k}+\mathbf{q})]}{E^i(\mathbf{k}) - E^j(\mathbf{k}+\mathbf{q})}$$

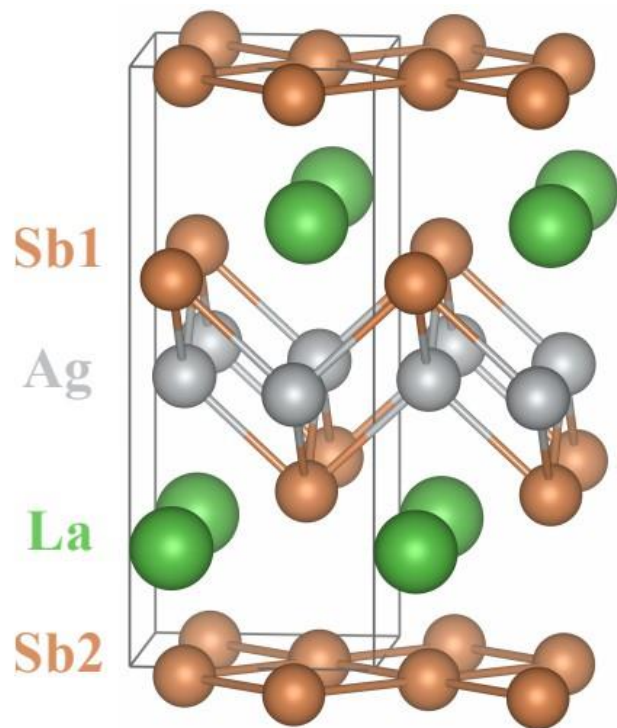
$R\text{Te}_3$ - nesting behind CDW



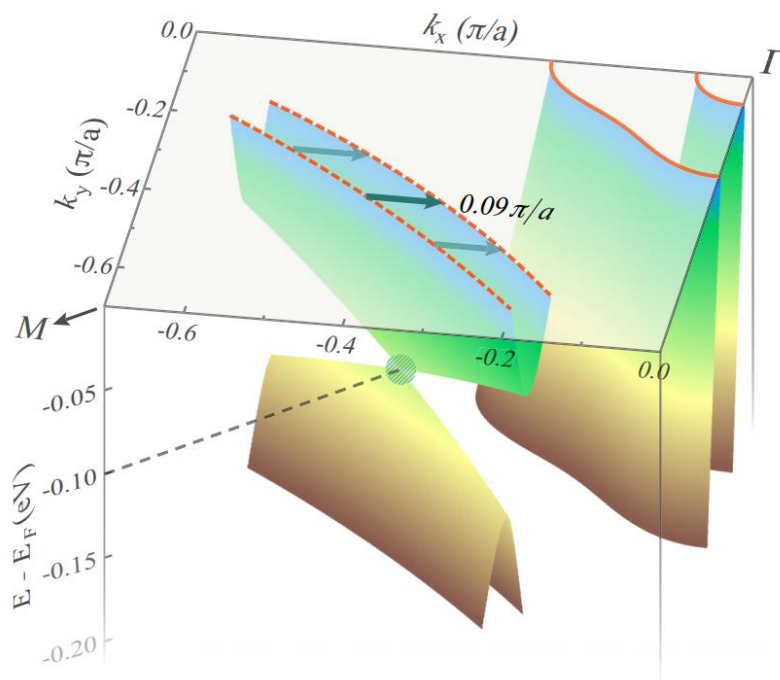
interband susceptibility



[A. Bosak et al., Phys. Rev. Res. **3**, 033020 (2021)]

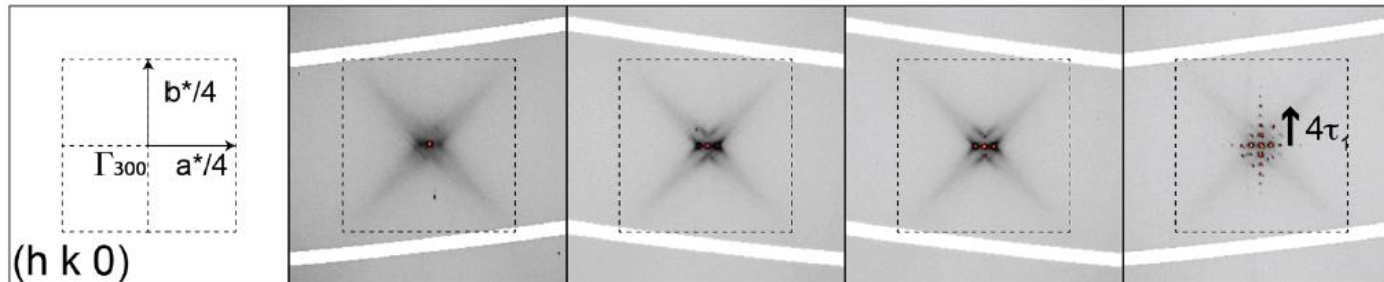


[X. Shi, P. Richard, K. Wang, M. Liu, C.E. Matt, N. Xu, R.S. Dhaka, Z. Ristic, T. Qian, Y.-F. Yang, C. Petrovic, M. Shi, and H. Ding, Observation of Dirac-like band dispersion in LaAgSb₂, Phys. Rev. B **93**, 081105 (2016)]



Diffuse scattering in LaAgSb_2

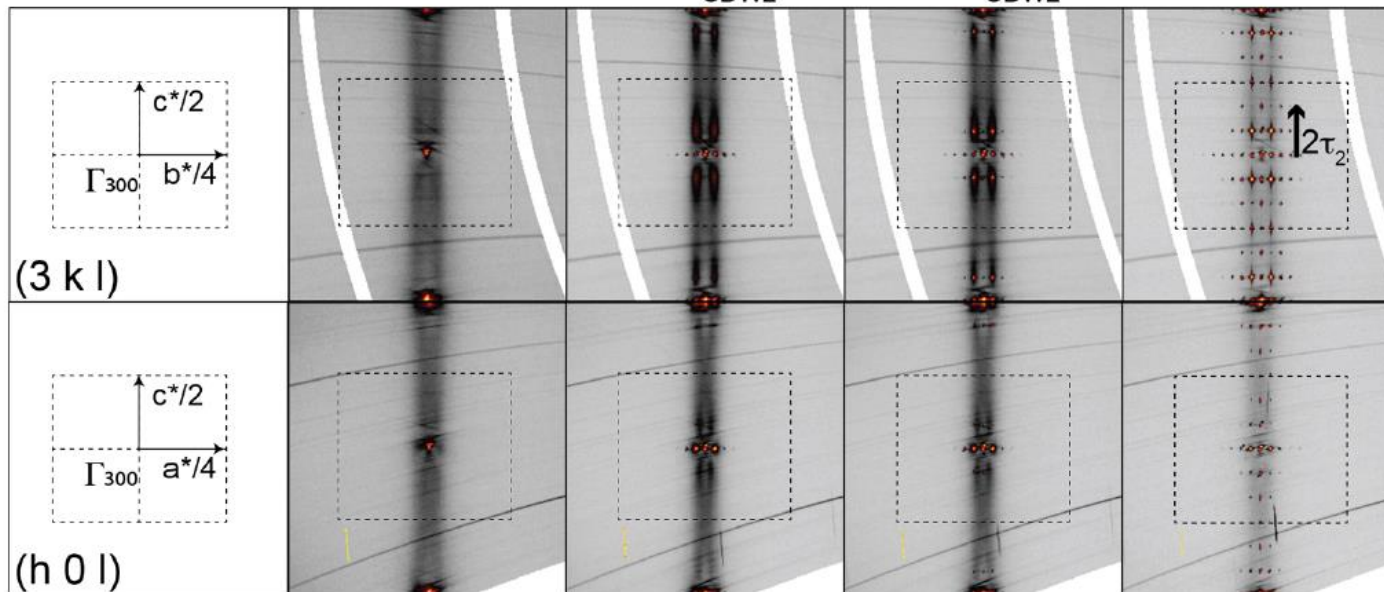
$T = 295 \text{ K}$ $T = T_{\text{CDW1}} + \delta$ $T = T_{\text{CDW1}} - \delta$ $T = 100 \text{ K}$



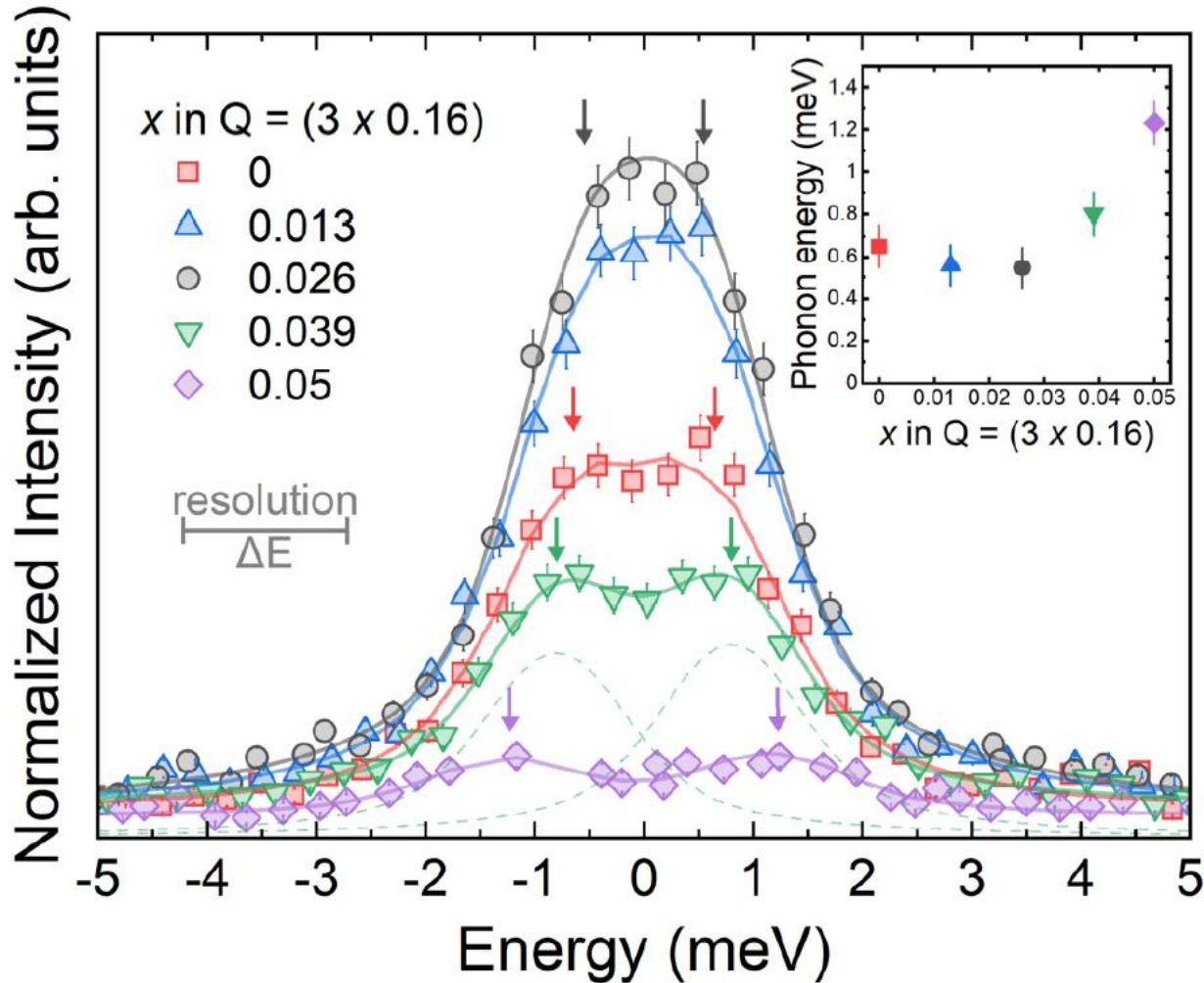
to CDW satellites
up to 7th order

diffuse tubes
with $\kappa_x \sim 30 \text{ nm}$

$T = 295 \text{ K}$ $T = T_{\text{CDW2}} + \delta$ $T = T_{\text{CDW2}} - \delta$ $T = 100 \text{ K}$



$$\tau_1 \sim 0.026 a^* \quad \tau_1 \sim 0.026 a^* + \tau_2' = 1/6 c^*$$



Diffuse features are inelastic

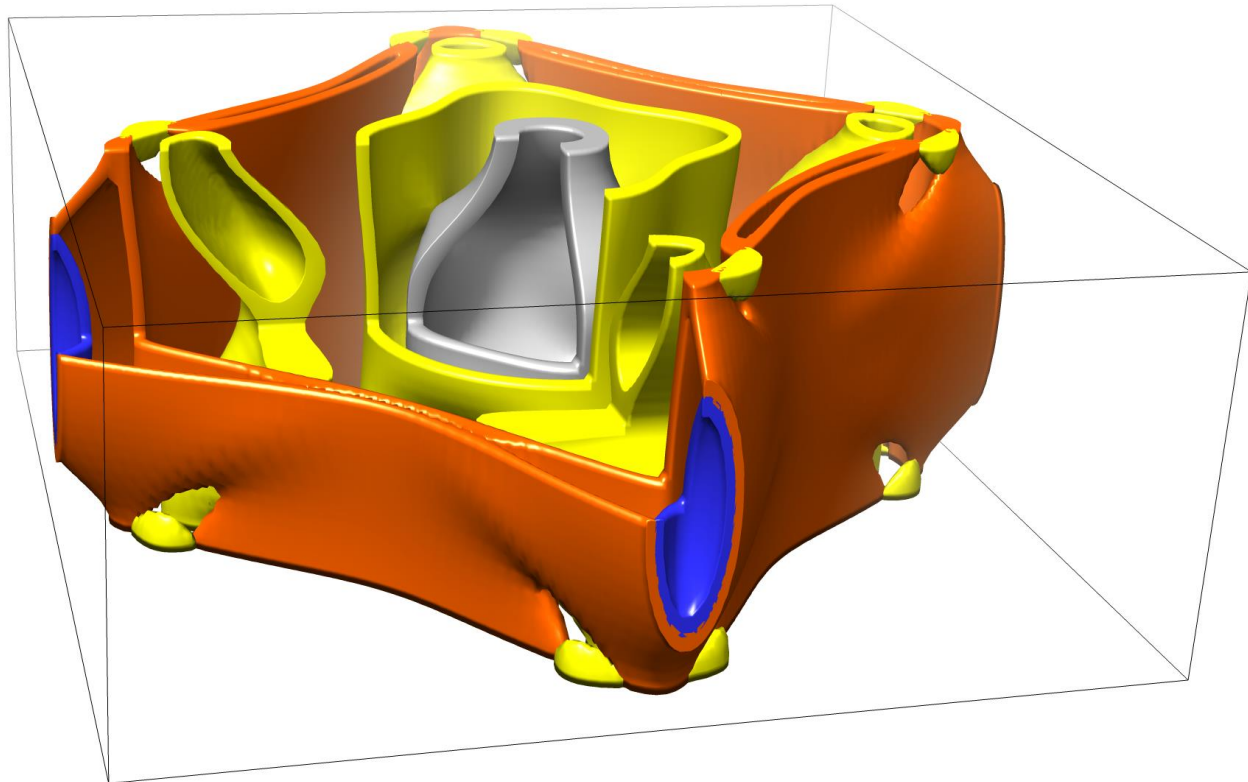
True Kohn anomaly

Soft phonon mechanism

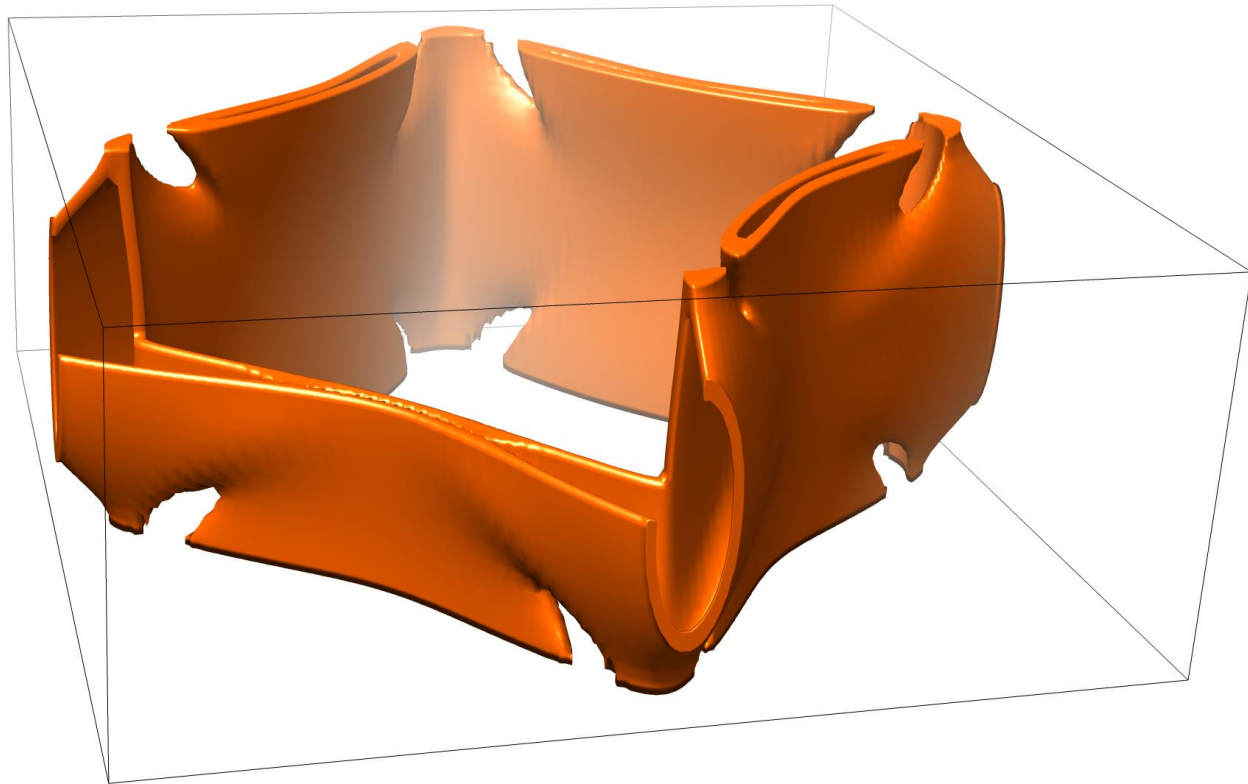
What is behind?

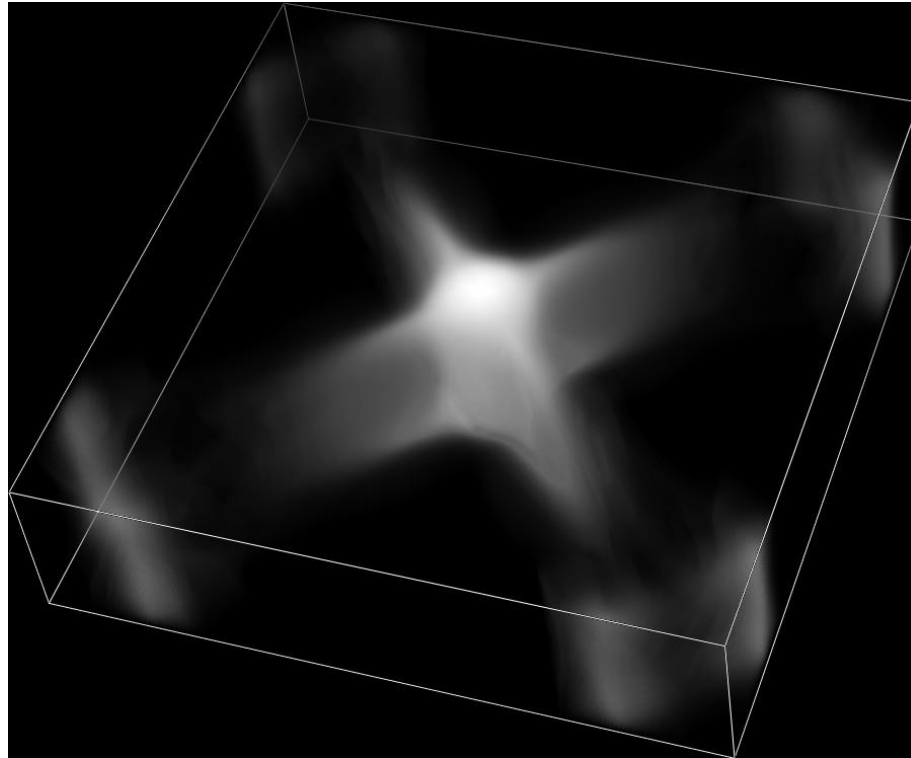
$$\tau_1 \sim 0.026 a^* + \tau_2' = 1/6 c^*$$

4 bands



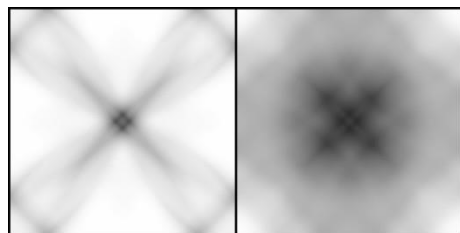
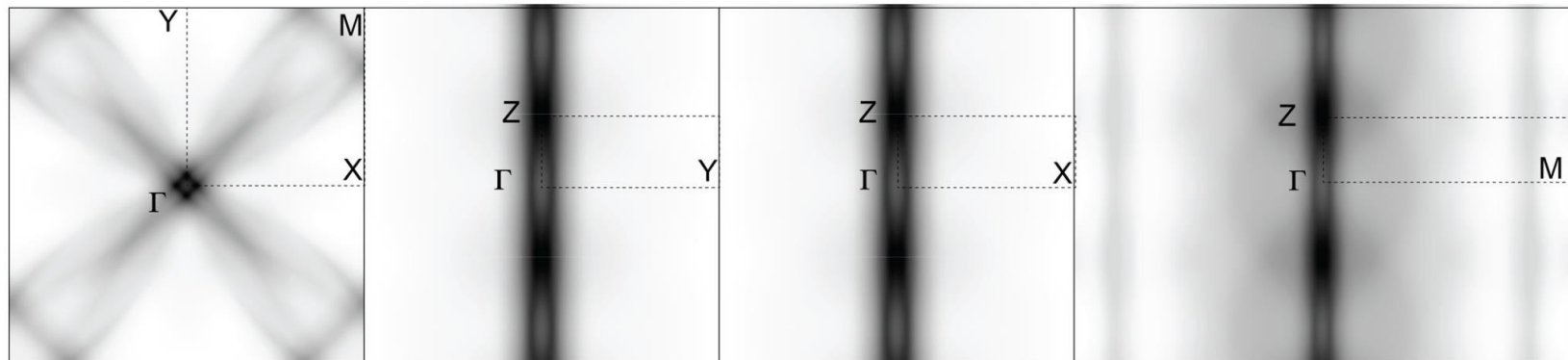
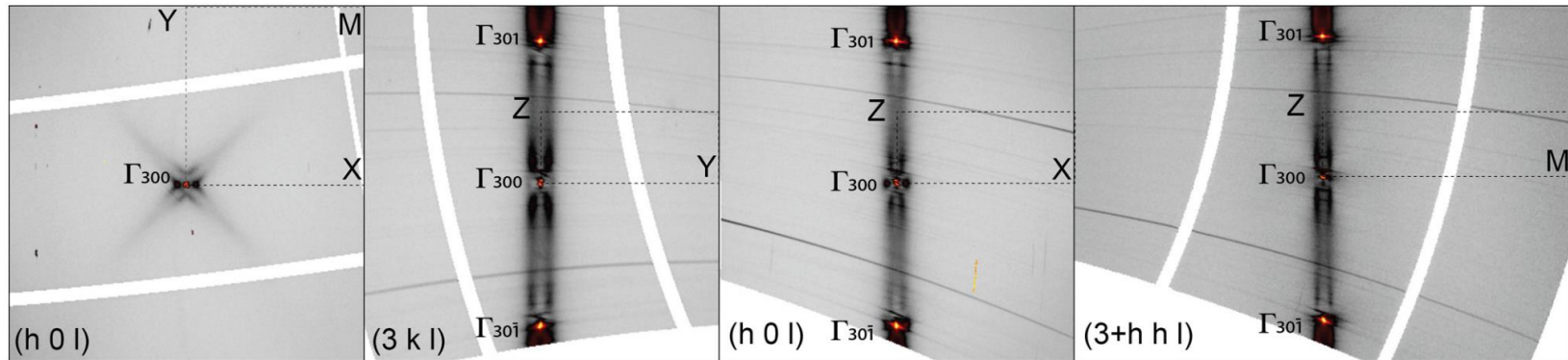
1 “good” band





$$\chi^{ij}(\mathbf{q}) = \sum_{\mathbf{k}} \frac{n_F[E^i(\mathbf{k})] - n_F[E^j(\mathbf{k}+\mathbf{q})]}{E^i(\mathbf{k}) - E^j(\mathbf{k}+\mathbf{q})}$$

Nesting behind transitions



χ_{33} χ_{total}

All band contributions are equal, but some band contributions are more equal than others

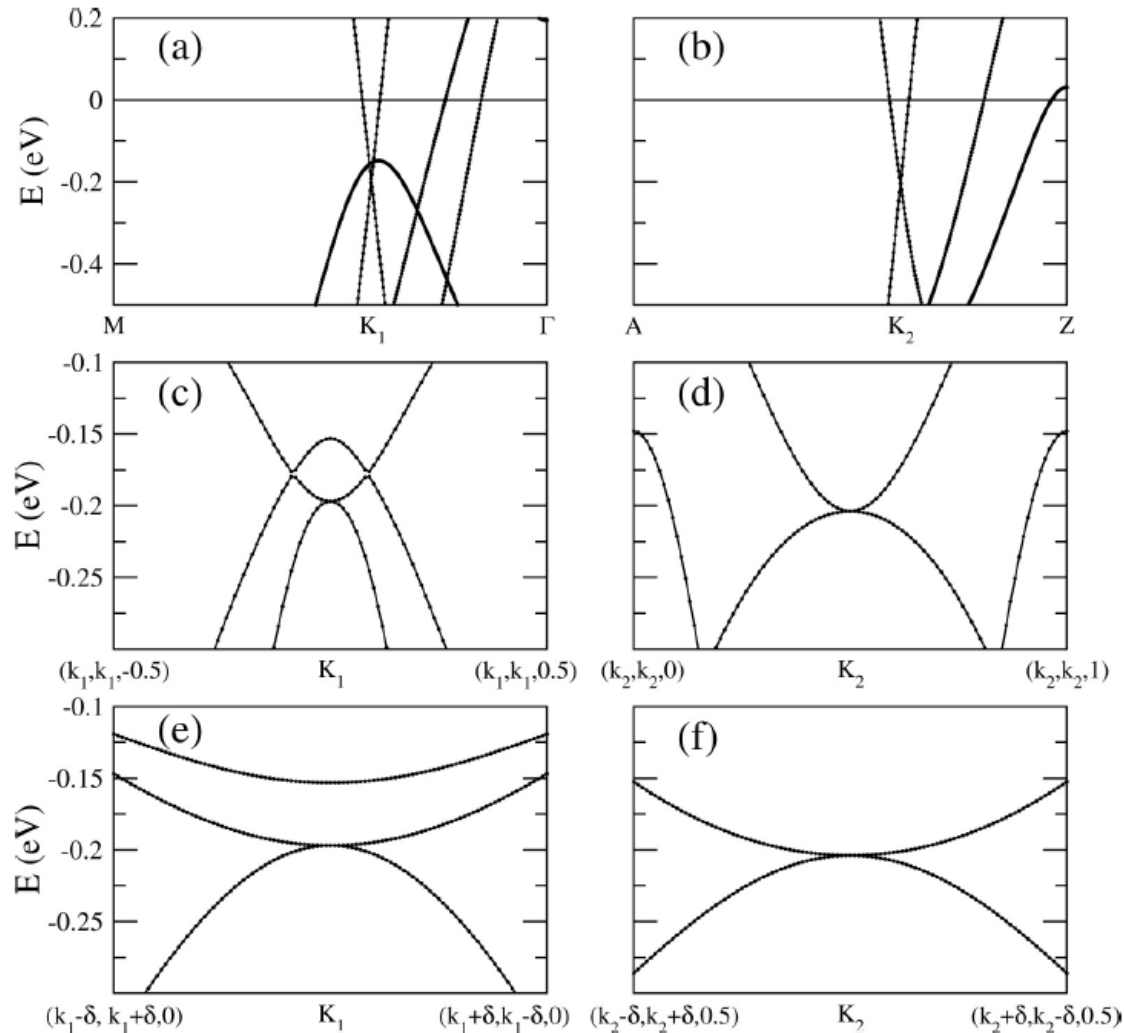


FIG. 8. Electronic band structure of LaAgSb_2 in the vicinity of the Dirac-type points. Band crossings with linear dispersive bands appear along the high-symmetry lines $M-\Gamma$ and $A-Z$ at points (a) $K_1 = (k_1, k_1, 0)$ with $k_1 = 0.1920$ and (b) $K_2 = (k_2, k_2, 0.5)$ with $k_2 = 0.2028$, respectively. (c) Band dispersion along parallel to the z axis across K_1 (c) and K_2 (d), and along an orthogonal direction in the xy plane ($\delta = 0.05$).



[with P. Rodiere, M. Leroux]

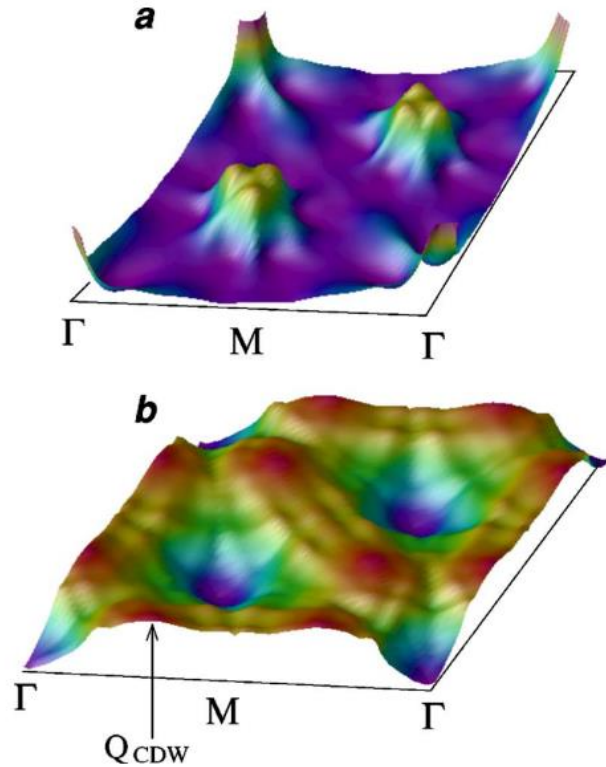


FIG. 5. (Color online) The noninteracting susceptibility of NbSe₂. (a) The imaginary part exhibits FS nesting driven peaks at $\mathbf{Q}=(\frac{1}{3}, \frac{1}{3}, 0)$. The plane at the bottom is a guide for the eye and corresponds to the lowest value of $\text{Im}\chi_0$. (b) The real part has very weak peaks at $\mathbf{Q}_{CDW}=(\frac{1}{3}, 0, 0)$ that come from energy intervals away from E_F (see text). The plane corresponds to the lowest value of $\text{Re}\chi_0$, which is also the density of states at the Fermi level.

[Johannes et al., PRB 73, 205102 (2006)]

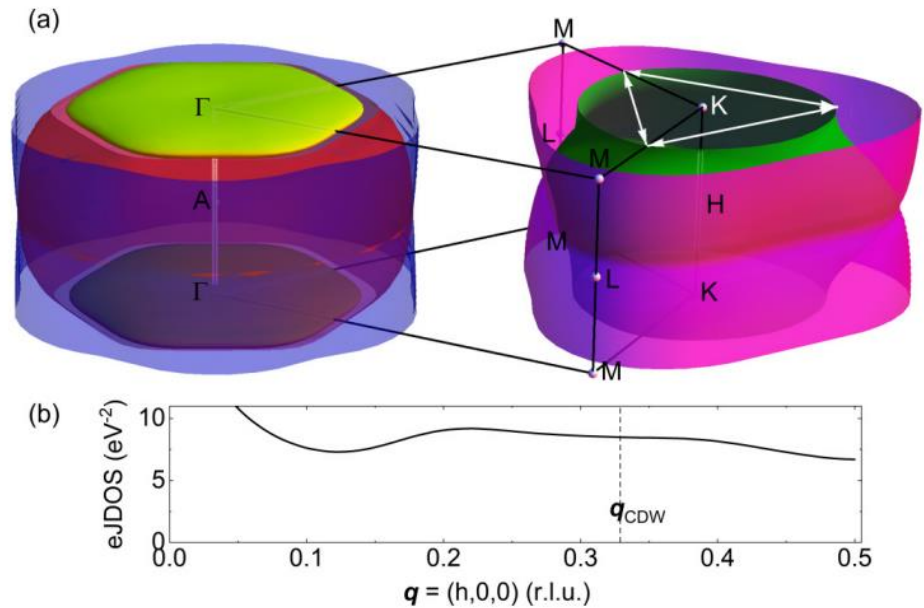
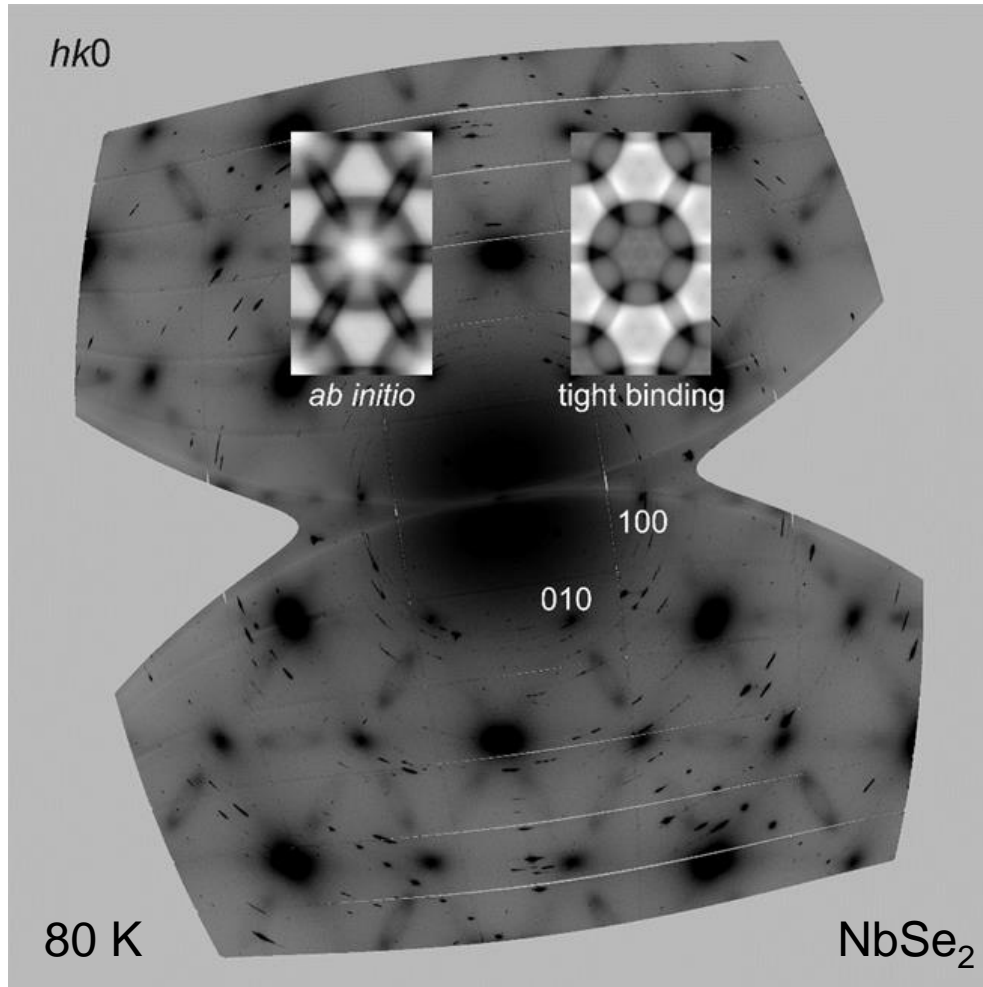


FIG. 4. (a) Calculated 3D FS. Capital letters denote high-symmetry points of the Brillouin zone. White arrows connect parts of the inner K pocket, where nesting was proposed [14] and CDW hotspots were reported [15]. (b) Calculated electronic joint density of states (eJDOS) corresponding to the FS shown in (a).

[Weber et al., PRB 97, 235122 (2018)]

$NbSe_2$ – nesting behind CDW

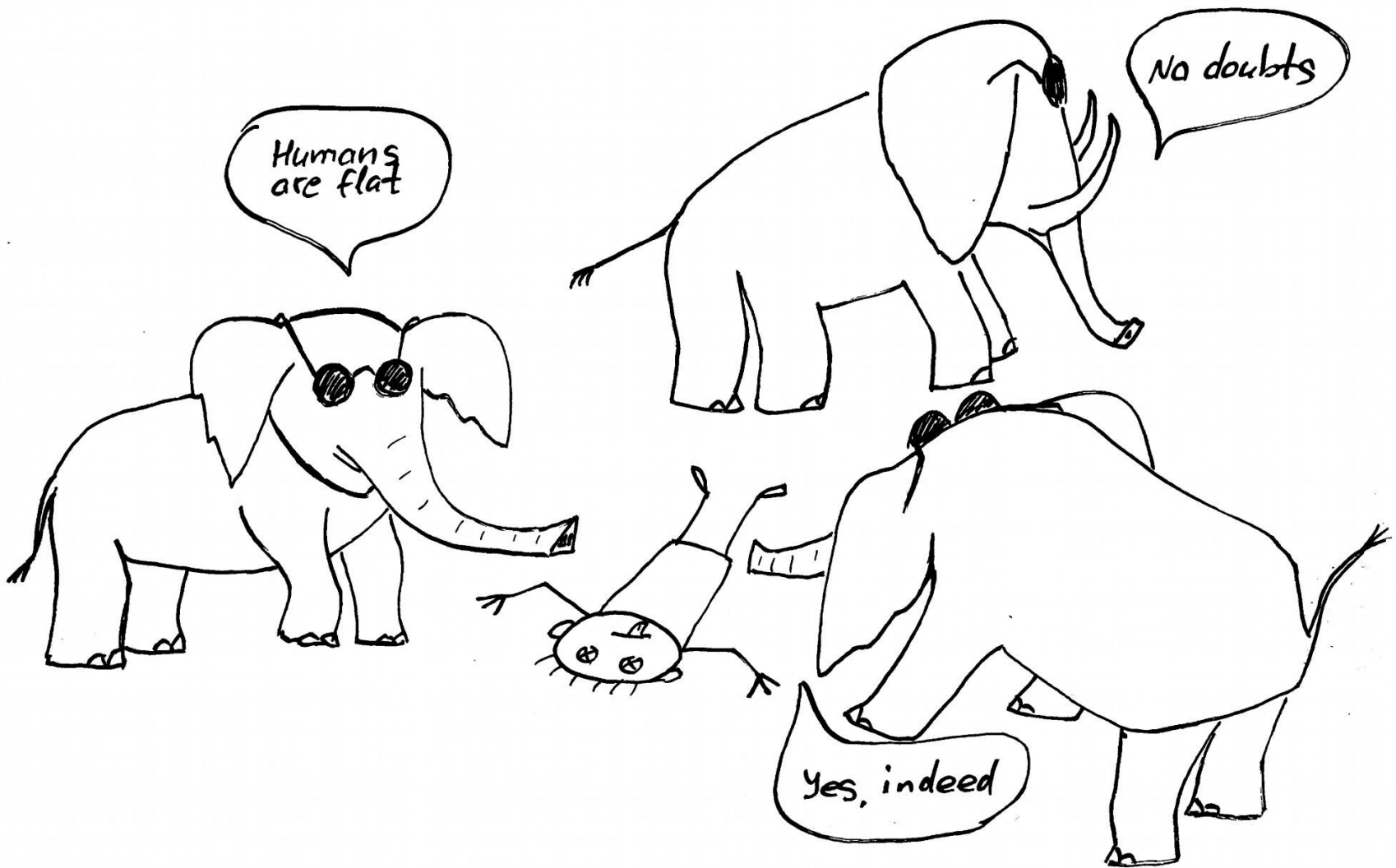


OK, no clear features at q_{CDW} in total χ

High degree of similarity for selected interband nesting

Not only q_{CDW} is reproduced, but 2D/3D shape of Kohn anomaly

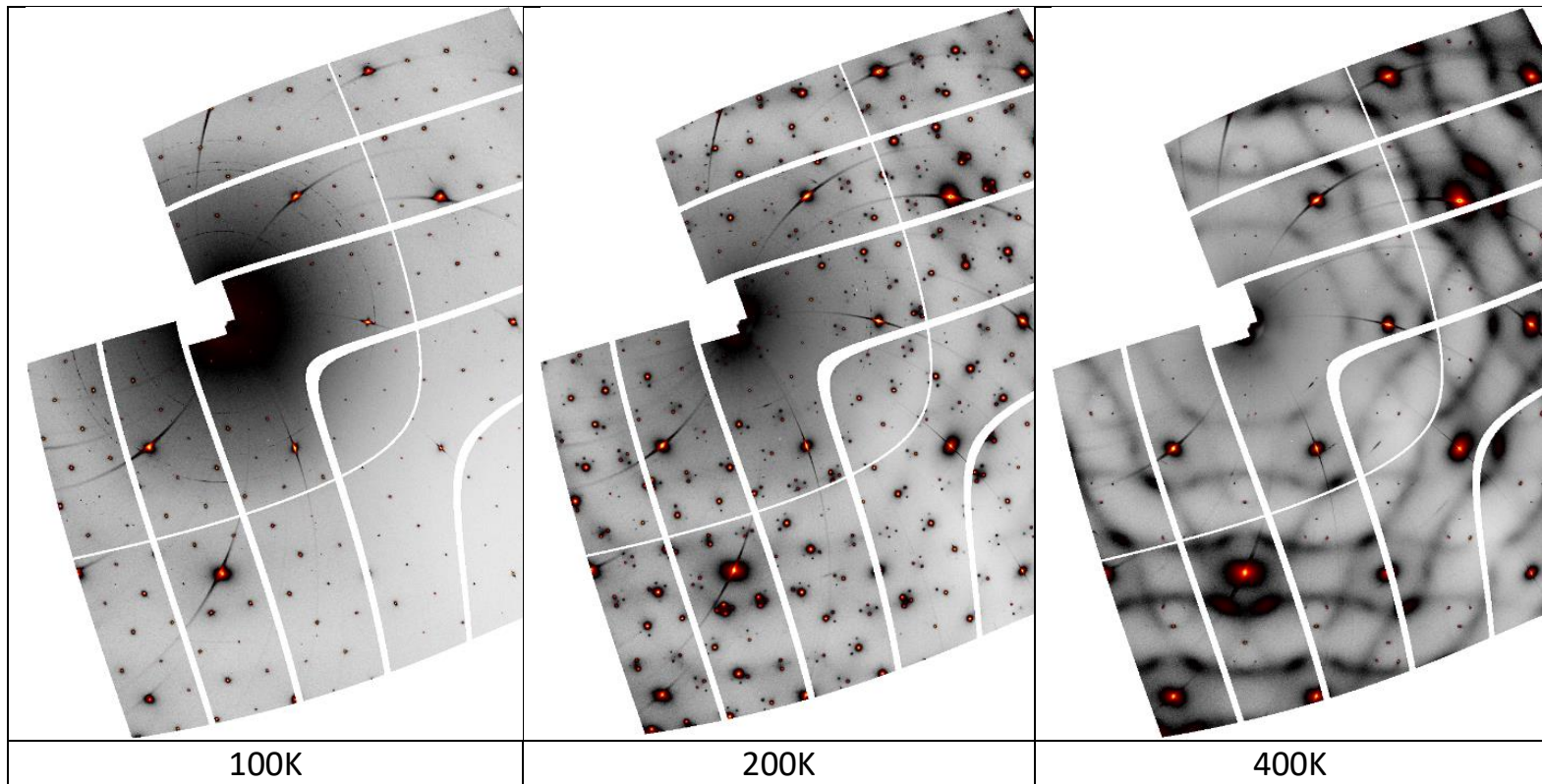
Biased views





[with J. Geck, A. Korshunov]

TaS_2 – no nesting behind CDW



- Nice background of soft phonons responsible for CDW transition
- No nesting can be taken responsible for this softening

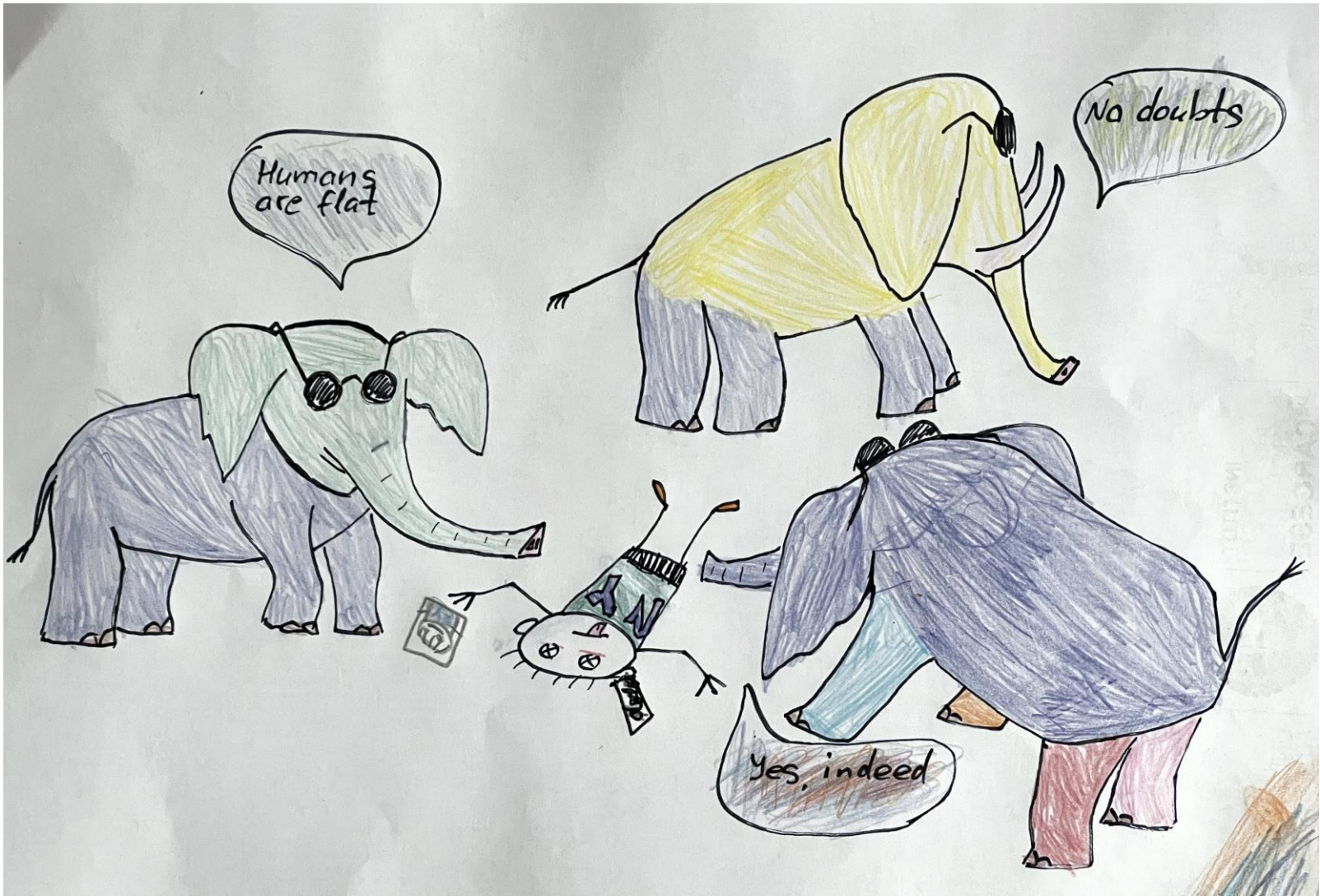
- DS helps to locate soft phonon features beyond of simple spots
- DS shape is more discriminating than just q_{CDW}
- Nesting and EPC are NOT mutually excluding
- It helps to combine DS with IXS
- (ID28 ESRF beamline offers tandem use of methods)



TOMORROW

A mystical land where 99% of all human productivity, motivation and achievement is stored.

proposal submission deadline 12.09.2022



[A. Bosak, V. Bosak, 2022]

Zinc Fermi surface and nesting picture

